Dynamic contrast enhanced magnetic resonance imaging: A review of its application in the assessment of placental function

Mathilde Jacquier, Chloé Arthuis, David Grévent, Laurence Bussières, Charline Henry, Anne-Elodie Millischer-Bellaiche, Houman Mahallati, Yves Ville, Nathalie Siauve, Laurent Salomon

*** Title Page and Abstract**

Title Page

Full title: Dynamic contrast enhanced magnetic resonance imaging: a review of its application in the assessment of placental function

Mathilde Jacquier [a,b], Chloé Arthuis [b,c], David Grévent [b,d], Laurence Bussières [a,b], Charline Henry [b], Anne-Elodie Millischer-Bellaiche [b,d], Houman Mahallati [e], Yves Ville [a,b], Nathalie Siauve [f,g], Laurent J. Salomon [a,b]

[a] Obstetrics and Gynecology Department, Assistance Publique - Hôpitaux de Paris, Hôpital Necker - Enfants Malades, 149 rue de Sèvres, 75015 Paris, France

[b] EA FETUS 7328 and LUMIERE Unit, Université de Paris

[c] Obstetrics and Gynecology Department, CHU Nantes, 38 Boulevard Jean Monnet, 44000 Nantes

[d] Radiology Department, Assistance Publique - Hôpitaux de Paris, Hôpital Necker - Enfants Malades, 149 rue de Sèvres, 75015 Paris, France

[e] Department of Radiology, University of Calgary, Calgary, AB, Canada.

[f] Radiology Department, Assistance Publique - Hôpitaux de Paris, Hôpital Louis Mourier, 178 Rue des Renouillers, 92700 Colombes

[g] INSERM, U970, Paris Cardiovascular Research Center - PARCC, Paris, France

Corresponding author:

Pr Laurent J. Salomon, Obstetrics and Gynecology Department, Assistance Publique - Hôpitaux de Paris, Hôpital Necker - Enfants Malades, 149 rue de Sèvres, 75015 Paris, France

laurentsalomon@gmail.com ; 0033609687271

Abbreviations:

AIF: Arterial Input Function The concentration of a tracer, in this case gadolinium based contrast agent, in blood/plasma over time.

ASL: Arterial Spin Labeling, an MRI technique used to measure blood flow in which contrast agents are not needed, but rather magnetic pulses are used to label blood as it flows into the area of interest.

BOLD-MRI: Blood Oxygen Level Dependent, a non-invasive in-vivo technique of placental oxygenation assessment using hemoglobin as an endogenous contrast agent.

DCE-MRI: Dynamic Contrasted Enhanced Magnetic Resonance Imaging MRI technique in which an exogenous intravascular contrast agent is administered and the passage of this contrast agent through tissues is dynamically imaged by obtaining serial images over time.

ED: Embryonic Day

EPI: Echo planar imaging

FBV: placental fractional blood volume

GCTT: Gamma capillary transit time, a mathematical model used to calculate functional MRI parameters

Gd-CA: Gadolinium-based contrast agents

HPZ and LPZ: high-flow zone and low-flow zone, two functional spaces of the murine placenta

IVIM: Intravoxel Incoherent Motion: MRI techniques in which attempts are made to account for the signal contributions from all motion at microscopic levels, namely perfusion at microvascular levels as well as diffusion into tissues, and provides information about tissue microcirculation and also diffusion related to tissue microstructure.

PBF: Placental blood flow (F=mL/min/100mL)

PS: Permeability surface area (mL/min/g)

SPIO: Super Paramagnetic Iron Oxides

T1-FFE: Fast Field Echo; FLASH: Fast Low Angle Shot; SPGR: Spoiled Gradient Recalling imaging: MRI sequences using gradient-spoilers destroying the residual transverse magnetization to optimize T1-weighting.

Vb: Fractional blood volume (%)

T1W images: T1 weighing of an image, is one in which the differences in tissue contrast is displayed on images based largely on the difference in T1 relaxation times of tissues. Such images are one of the fundamental methods of displaying MRI images and can be acquired using a broad spectrum of MRI sequences

DW imaging: Diffusion-weighted magnetic resonance imaging is a form of MR imaging based upon measuring the random Brownian motion of water molecules within a voxel of tissue.

SNR : Signal to noise ratio

CNR : Contrast to noise ratio

CA : Contrast agent

Abstract:

It is important to develop a better understanding of placental insufficiency given its role in common maternofetal complications such as preeclampsia and fetal growth restriction.

Functional magnetic resonance imaging offers unprecedented techniques for exploring the placenta under both normal and pathological physiological conditions. Dynamic contrast-enhanced magnetic resonance imaging (DCE MRI) is an established and very robust method to investigate the microcirculatory parameters of an organ and more specifically its perfusion. It is currently a gold standard in the physiological and circulatory evaluation of an organ.

Its application to the human placenta could enable to access many microcirculatory parameters relevant to the placental function such as organ blood flow, fractional blood volume, and permeability surface area, by the acquisition of serial images, before, during, and after administration of an intravenous contrast agent. Widely used in animal models with gadolinium-based contrast agents, its application to the human placenta could be possible if the safety of contrast agents in pregnancy is established or they are confirmed to not cross the placenta.

***Highlights**

Highlights

1. DCE-MRI is a very robust method to investigate the microcirculatory parameters.
2. DCE-MRI provide extraordinary range of data on the placental function.
3. The future of DCE-MRI lies in the widespread availability of safe contrast agents.
4. Perspectives can be envisaged with the combination of several functional-MRI techniques.

***Manuscript References**

Manuscript

Introduction:

The current challenge in placental imaging is to improve our knowledge of its function. One of the essential parameters of the placental function is its perfusion. A more precise understanding of placental perfusion is of great interest as under-perfusion or placental insufficiency, could result in intrauterine growth restriction or perinatal death [1-3]. The study of placental permeability is also of great importance, since the placenta is the only organ that allows the exchange between the mother and the fetus. Altered permeability could be a key factor in placental pathophysiology in the event of insufficient transfer of nutrients to the fetus [4-7].

An approach to placental function can be achieved by ultrasound, a tool used as first line in current practice but remains limited in the assessment of the intervillous space and uteroplacental circulation. Various functional placental MRI techniques have been developed for two decades. All aim at providing information on placental perfusion, sometimes only semi-quantitatively (IVIM), but only one, covered in this review, allows quantitative characterization of both perfusion and other functional parameters such as permeability and fractional blood volume: Dynamic Contrast Enhanced Imaging (DCE). DCE MRI is an established and very robust method to investigate the microcirculatory parameters of an organ, including ~~and more specifically~~ its perfusion. It is currently a gold standard in the physiological and circulatory evaluation of an organ. Its application to the human placenta could enable to access many microcirculatory parameters relevant to the placental function.

Often criticized for its complexity, we initially hope to clarify the basics of this technique. We will then discuss the different contrast agents available, followed by a review the main results it provides on the fundamental parameters of placental functionality: perfusion, permeability and fractional blood volume. Finally, we discuss potential future applications of this technique.

Fundamentals

Basic concept of DCE-imaging

DCE-MRI is based on the analysis of tissue enhancement kinetics after intravenous injection of a contrast agent. Serial T1-weighted acquisitions are carried out throughout the intravenous injection of a contrast agent : 1) Anatomical un-enhanced images are acquired before injection to obtain base-line signal values in the vasculature and tissues in the regions of interest 2) Images are acquired as the bolus of contrast agent first arrives in the arterial system allowing demonstration and calculation of an Arterial Input Function (AIF) 3) Finally, images are acquired as the contrast agent passes through and washes out of tissues and tissue enhancement fades and reaches a steady state (Figure 1) [8-10].

The kinetics of tissue enhancement reflects two basics physiological phenomena: the tissue perfusion and the leakage of the CA into the interstitial space described in detail by Cuenod and Balvay [11].

The tissue enhancement kinetics give us information about several physiological parameters of the microcirculation (Figure 2). The initial rise of the curve depends on the tissue ~~perfusion~~ blood flow ~~rate~~, that is to say the ~~tissue blood~~ flow entering and exiting a volume of tissue (FT, expressed in mL of blood/min/100 mL tissue). FT corresponds to the ambiguous term of "perfusion". Then, the early peak reflects the tissue blood volume (also referred to as blood volume fraction) which corresponds to the volume of capillary blood contained in a certain volume of tissue (Vb, mL blood/100 mL of tissue or in %). The kinetics after the peak depend on the permeability, the flow of molecules through the capillary membranes in a certain volume of tissue (surface area product PS, in mL/min/100 mL tissue). Finally, the later part of the curve depends on the tissue interstitial volume, also known as the extravascular and extracellular volume fraction (Ve, %). [11, 12].

DCE-MRI acquisition: basic protocol, data pre-processing and optimizations

Fast gradient echo T1-weighted sequences are mostly used with gradient-spoilers destroying the residual transverse magnetization (T1-FFE, FLASH, SPGR, RF spoiled FE).

The parameters of these sequences (low flip angle, short repetition time, increased receiver bandwidth) are associated with a low SNR (signal to noise ratio). Considering that SNR has a very important influence on DCE-MRI pharmacokinetic modeling, with higher SNR increasing

the precision with which parameters can be evaluated [13], enhancing SNR is of great importance. Choosing the optimal flip angle is found by many authors [13-16] to be one solution to obtain a higher SNR. A compromise between spatial–temporal resolution, SNR and CNR (contrast to noise ratio) remains a major challenge.

Unlike in DCE-CT, enhancement values and concentration of contrast agent do not follow a linear relationship in DCE-MRI. Many strategies have been developed to improve this conversion and are summarized by Cuenod [11].

Contrast agents:

The contrast agent (CA) is considered to have the properties of a tracer, that is to say it does not modify either the volumes of the compartments over time or the physiological conditions of the system. The mixing of a CA is considered instantaneous and homogeneous inside each compartment. MRI contrast agents may be categorized according to their magnetic properties, chemical composition, route of administration, effect on the magnetic resonance image, biodistribution and application. Their classification and application have been the subject of a review by Xiao [17].

Conventional use of Gadolinium based contrast agent (Gd-CA) in clinical practice:

Gadolinium chelates are paramagnetic contrast agents that shorten T1 and T2 relaxation times. Their placental pharmacokinetics in animal models are well established: a placental wash-out has been quantified at 50% one hour after injection in rabbits and at 99% 24 hours after injection in rats [18,19]. In the human placenta, only qualitative data describe an early placental enhancement with a quick wash-out compared to the myometrium [20]. Gadolinium

chelates then reach the fetal blood and are excreted through the urine in the amniotic fluid [18]. This accumulation in the amniotic fluid is poorly documented. Possible reabsorption in the fetal lungs or digestive tract [18] raises concerns of potential toxicity [21,22]. Although the administration of Gadolinium appears safe in the first trimester [22, 23], a large epidemiological study by Ray et al [22] of over 1.4 million deliveries in Canada suggested that exposure during the second and third trimesters may carry greater risks of rheumatologic-inflammatory like conditions (adjusted hazard ratio, 1.36; 95% confidence interval [CI], 1.09–1.69) and stillbirth or neonatal death (adjusted relative risk, 3.70; 95% CI,

1.55–8.85). Despite undisputed strengths, this large registry study lacks relevant clinical history, including co-morbidities and the indications for performing the MRI studies in pregnancy. MRI studies would have been performed in pregnancy for specific clinical indications, including: (i) early and unknown pregnancy, therefore increasing potential adverse consequences, and (ii) maternal-fetal conditions necessitating MRI despite the pregnancy. Fraum et al [24] summarized the international guidelines regarding the use of Gd-CA in pregnancy: the current consensus is to restrict its use to cases where the maternal-fetal benefits outweigh the potential risks after a case-by-case analysis.

Alternative contrast agents used in research

To overcome the uncertainty about gadolinium safety [21,22], other contrast agents that remain in the intravascular space have been developed. Establishing their safety and widespread use is the main challenge to the generalization of the use of the DCE-MRI in human pregnancy in the coming years. The principal characteristics of Gd-CA, liposomal-Gd and SPIO agents are summarized in table 4. Other contrast agents such as manganese complexes have also been developed [25].

Liposomal gadolinium [26-36]

Liposomal-Gd agents have important biological and physical characteristics distinguishing them from common GBCA: (1) a large size (100–150 nm diameter, molecular weight~ 2 Å~ 105 kD) gives them a long in vivo half-life and a low propensity to extravasate [26-28] and (2) a high T1-relaxitivity [29-31]. These properties result in an extended imaging window for acquisition of high-resolution images rich in SNR and CNR [32]. Liposomal-Gd contrast agents have different molecular structures, typically either core-encapsulated nanoparticles (encapsulated gadolinium within the core-interior) or surface-conjugated nanoparticles (gadolinium conjugated on the surface). Ghaghada described a Dual-Gd agent (a nanoparticle that has both core-encapsulated and surface-conjugated gadolinium), with improved SNR and CNR [32]. It has been demonstrated that liposomal-Gd does not penetrate the placental barrier in animal models [32-36]. In 24 normal-growth feto-placental units, Badachape [36] reports the ability of liposomal-Gd contrast agents to provide an accurate estimation of placental fractional blood volume (FBV) with increasing values as gestation progresses. To our knowledge, there is no data about their use in human placenta,

and maternal and fetal safety remains to be established. This contrast agent could have the advantage of quantifying only maternal perfusion into intervillous space. However fetal pharmacokinetics or placental permeability may not be evaluated by this type of contrast agent.

SPIO (Super Paramagnetic Iron Oxides) [37-41]

Iron oxide nanoparticles were first developed for the treatment of anemia and have recently received substantial interest as an MRI contrast agent due to their T1 and T2 relaxation time shortening properties. Unlike Gd-CA, Ferucarbotran and Ferumoxytol, the two main such agents, have a long intravascular half-life (14h for ferumoxytol vs 1.6h for Gd-CA), which results in a long blood pool phase prior to detectable contrast extravasation. Several studies have shown that neither Ferucarbotran nor Ferumoxytol cross the placental barrier [39-41]. Ferucarbortran-enhanced MRI was used by Deloison et al [41] who showed its capacity to measure placental perfusion ~~and permeability~~ in both physiological and pathological settings in a rat model of chronic hypoxia that led to intrauterine growth restriction (placental blood flow in the ligated horns compared to the normal horns (108.1 versus 159.4 mL/minute/100 mL, p = 0.0004)). Two studies [39,40] demonstrated the feasibility of ferumoxytol-enhanced MRI in pregnancy with a nonhuman primate model. ~~R2* mapping and quantitative susceptibility mapping in a pregnant nonhuman primate model.~~

Data Analysis

Enhancement data can be analyzed with qualitative, semi-quantitative or quantitative methods. These three approaches are described below in order of increasing complexity.

Qualitative analysis:

This is the most subjective method based on an operator's interpretation. Routinely used in breast imaging [42], the qualitative analysis consists of describing the enhancement by its intensity, its speed, and its homogeneous or heterogeneous appearance [9,43]. Although not quantitative, its simplicity gives it advantages (less sensitivity to variations in sequence parameters, no requirement in terms of calculation) [12].

Semi-quantitative analysis:

It consists of evaluating quantitative parameters from the time-intensity curve. Various parameters, including the maximum (relative) enhancement (%), the time to peak (in seconds), the rate of peak enhancement (%), the maximum slope of the curve fit function and the area under the curve (AUC), could be calculated for each ROI [44-46]. This analysis makes it possible to compare different placental perfusion profiles (i.e placental insufficiency) but does not, for example, provide a flow rate in mL/min/dL.

Quantitative analysis:

This method makes it possible to quantify the flow rate of the intervillous space, in order to establish reference values for a normal pregnancy at a given gestational age. This method must take into account that the contrast agent acts as a tracer and is therefore found simultaneously in the placenta and the fetus.

Models to evaluate flow rate have been established. They need the definition of an arterial input function (AIF) and must be adapted to the acquisition conditions.

AIF (arterial input function):

AIF is the estimation of the contrast agent concentration in an afferent artery as a function of time. A requirement of almost all quantitative analysis methods, a wide variety of strategies to measure it have been described. The most invasive one consists of introducing an arterial catheter to sample blood during the imaging process for later analysis [47-48]. Deemed impractical due to its invasive nature, simpler methods assume that the AIF is similar for all subjects [49], but the inter- and intrasubject variations in AIF leads to large systematic errors in the analyses [50-51]. The AIF can also be collected from the DCE-MRI data set; giving an accurate and individual AIF measure, this method requires the presence of a large vessel within the field of view, which is not always the case. If no vessel is available, a mean AIF corresponding to an average value obtained in a population can be used as described by Parker [52]. Finally, Yankeelov suggested a method of quantitative pharmacokinetic analysis of DCE-MRI data without knowledge of the AIF [53].

Design of the acquisition protocol depending on the desired parameters

The ability to study microcirculatory parameters depends on the acquisition conditions. Parameters about tissue blood volume and capillary permeability only require intermediate frame rates and acquisition time, whereas high temporal resolution and long acquisition time permit the study both perfusion and permeability parameters [11]. The acquisition protocol therefore must be designed according to the parameters studied.

Models

Given that MRI contrast agents acts as a tracer, to study and quantify blood flow a compartmental analysis is required. The placenta is considered as a two- or three-compartment organ comprising a tissue compartment, a blood compartment, and an interstitial compartment, depending on the organ and the species studied [54-56]. This is especially important for the placenta because different studies are comparing animal models and the mouse/rat placenta is quite different than the macaque/human placenta. Even though their overall function is the same, the compartments in these different species are quite different.

The range of models available differ by their complexity. The more complex the model, the more it closely follows physiology, with an unfortunate decrease in accuracy. Initial models described, the Tofts-Ketty model and Brix model [59-60] have two-fittings parameters: Ktrans, the volume transfer constant between blood plasma and extravascular extracellular space (EES) and Ve, the volume of EES per unit volume of tissue. As these models are not suitable for analyzing data acquired with a rapid temporal resolution [11], other physiological models have emerged.

Thus, the three-compartment model analysis is based on the underlying physiological principle that the placenta is a countercurrent exchange system between the maternal and fetal compartments [61]. The maternal vascular compartment of the placenta is supplied by the arterial input (the uterine arteries) and drained by the venous output (Figure 3). The fetal vascular compartment of the placenta is directly connected to the fetus [62]. The

exchanges between compartments, governed by concentration gradients, are described using transfer constants according to the following equation:

$$dq2/dt = k(2.1) \cdot q1(t) - k(0.2) \cdot q2(t)$$

~~The concentration in the intravillous space depends on the amount in the general maternal circulation as well as the rates of arterial input and venous draining.~~ Exchanges between compartments (q1: arterial input, q2 and q3: maternal and fetal compartment of the placenta, q4: fetus) are governed by concentration gradients (k). q represents the quantity of contrast medium of each compartment.

The steepest slope model, another quantitative model first described by Miles [63], is a gradient-based approach to quantify perfusion, based on the initial uptake phase of the contrast in the target organ. An arterial input function is defined, which is usually at the hilum of the kidney to avoid pulsation artifacts within larger blood vessels. After 3D-segmentation of the placenta and a baseline signal correction for each concentration time curve of the DCE image sequence, the tissue perfusion is quantified from the following equation [63]:

$$F = \max(C'(t)) / \max(AIF(t))$$

where (C'(t)) is the time-differential of the concentration-time curve, and AIF(t) is the previously defined arterial input function.

Another approach is the gamma capillary transit time (GCTT) model described by Schabel [64], a generalized impulse response model for DCE-MRI that mathematically unifies the Tofts-Kety, extended Tofts-Kety, adiabatic tissue homogeneity, and two-compartment exchange models. This is achieved by including a parameter ($\alpha-1$) representing the width of the distribution of capillary transit times within a tissue voxel. The GCTT model was utilized for analysis due to its ability to account for heterogeneity in intravoxel contrast reagent transit times [65].

Finally, based on the GCTT model, Frias et al. [65] developed an intervillous space segmentation to quantify blood flow within individually identified cotyledons and three-dimensionally maps the placental structure in a way that is consistent with the placental histopathologic structure.

Main results of the micro-circulatory parameters

Tissue blood flow (FT) and fractional blood volume (Vb) in normal physiological conditions

Despite heterogenous acquisition protocols, consistent results found a mean ± standard deviation FT value of 130 ± 50 mL/min/100 mL [67-68] and a mean maternal volume fraction (Vb) of 36.5% [67, 68] (Table 1).

Two studies have separated the analysis of perfusion between the functional compartments (HPZ and LPZ) of the placenta [69-70]. They found a significantly higher perfusion in the high-flow compartment (HPZ) compared to the low-flow compartment (LPZ) ($p < 0.002$). In fact, the caliber of the vessels and therefore the enhancement kinetics differ in those different regions. However, the perfusion trends of the whole placenta are similar to those seen when the placenta was studied by region. The data on the evolution of these two functional perfusion parameters with gestational age differ. While Yadav et al [70] found a statistically significant increase in perfusion of the whole placenta and HPZ ($p=0.02$ and $p<0.05$ respectively) as the pregnancy progresses, Remus et al [69] found no such statistically difference in either compartment at Embryonic Day (ED) 14.5 and ED16.5 ($p=0.103$ and $p=0.092$ respectively).

Unlike the murine model, the primate model shares essential placental anatomical features with the human model (hemochorial placenta and cotyledon structure), which makes this model particularly relevant. Frias et al [65] sought to develop a model as close as possible to the histopathological structure of the placenta and successfully developed a DCE-MRI protocol in primates that quantifies blood flow in individually identified cotyledons. They found a mean ± SD volumetric flow rate through each perfusion domain of 27.5±10.0 mL/min with considerable variation (from 9.03 to 44.9 mL/min).

Tissue blood flow (FT) and fractional blood volume (Vb) in pathological conditions

Pathological conditions that decrease placental blood flow can be induced either by exogenous means including pharmacological models [71], biological models [72] and surgical models [68,73], or by endogenous ones [74, 76].

The comparison of placental blood flow (PBF) between pathological groups and controls have been investigated in seven studies [41, 68, 71-75] (Table 2). Two studies [71,73] reported a decreased PBF in the pathology group ($p<0.001$ and $p=0.0012$ respectively) while Lemery et al [72] found no difference in a L-NAME model reproducing preeclampsia-like

conditions (p = 0.496). Interestingly, Remus et al [74] found an early decrease in PBF in a group exposed to acoustic-stress at ED14.5 (123±21 vs 147±31 mL/min/100 mL; p. 0.04) followed by a subsequent increase to ED 16.5 (192 ± 51 vs 141 ± 29 mL/min/100 mL, p. 0.001). This suggests that compensatory mechanisms could be involved. In this regard, three studies [77-79] all show a decrease in vessel density in the labyrinthine zone in early pathological states (ED 14.5) followed by a subsequent increase in vessel density to ED16.5 [41,42]. In a L-NAME model of placental hypoperfusion, Tarrade et al [79] found another compensatory mechanism with an increased proportion and surface density of maternal blood space in the L-NAME groups. The different models are therefore able to highlight differences in perfusion in the pathology groups compared to the control groups.

Permeability:

DCE-MRI offers the unique possibility to assess placental permeability, that is to say is the flow of molecules through the capillary membranes in a certain volume of tissue (mL/min/100 mL tissue). The evaluation of the permeability is particularly interesting for therapeutic studies or to evaluate the transfer of viruses or nutrients for example. Also called the surface area product (PxS), it can be characterized by the influx volume transfer constant Ktrans (min−1), equal to the product of the transfer constant and the blood volume [80]. Several models to assess permeability have been developed, some neglecting the tissue blood volume [81, 48, 59], other taking it into account (the extended Kety or Tofts General Kinetic Model (GKM) [82]. Other models are able to assess both perfusion and permeability [80, 83]. To our knowledge, only one study reported results about placental permeability, which were obtained with a dual-echo MR imaging sequence [67]. However, this type of analysis requires a high volume of injected contrast agent [62]. We are particularly interested in assessing placental perfusion and not placental permeability in placental insufficiency. Thus, contrast agents remaining only in the maternal intervillous space would provide significant clinical information with safety.

Human application

MR Imaging of placenta accrete spectrum ~~disorders~~ (PAS) [84-101]

Previous studies using DCE-MRI in humans have focused on the assessment of PAS, without describing quantitative parameters of perfusion [84-87]. Millischer et al [84] demonstrated that a Gadolinium injection improves the ability of radiologists with the diagnosis of placenta accreta with MRI. Liposomal-Gadolinium also appears to be of great interest, enabling adequate visualization of the retroplacental clear space [36]. Romeo has shown, however, that the simple use of non-contrast MRI, combined with ultrasound assessment of placental adhesion spectrum (PAS), increased its probability of detection from 80 to 91% [88]. A recent systematic review by Kappor [89] classifies MRI signs of PAS and highlights best practice guidelines for imaging diagnosis of PAS. This will be covered in a separate article dedicated to placental anatomy in this special issue.

MR Imaging of human placental perfusion

To our knowledge, only one study has demonstrated that the evaluation of human placental perfusion by DCE-MRI is feasible. The Placentimage trial [102] evaluated in vivo placental perfusion parameters in pregnant women undergoing termination of pregnancy between 16 and 34-weeks gestational age (GA). The mean value of the placental blood flow (FT) was 137 mL/min/100mL, concordant with the results obtained in human pregnancies by isotope techniques [103] (110 mL/min/100 mL) and by echo planar imaging sequences (EPI) [104] (176 + 24 mL/min/100 mL). FT decreased with gestational age, halving between the beginning of the 2nd trimester and the end of the 3rd trimester, related to the growth of the placenta, villous maturation, and to decreased placental efficiency over gestation (p=0.011). The results also suggested that the FT and Ftotal values estimated by DCE-MRI in human pregnancies could detect placental dysfunction with a tendency towards decreased values in IUGR compared to non-IUGR fetuses (p=0.07 and p=0.0008, respectively). This work also explored in vivo fractional blood volume, finding Vb values of 61.77%. These results should be considered exploratory due to potential confounders such as different MRI sequences and platforms, technical limitations, image failures, and limited reproducibility between centers. However, this is the first study that has measured in vivo placental perfusion values in pregnant women using Gd based contrast agents.

Futures considerations

This review shows the extraordinary range of data that the DCE can provide on the placental function. It is the only technique capable of determining parameters of microcirculation other than perfusion for example, permeability [67]. The data provided are quantitative, at the cost of a certain complexity in the analysis of the data that are yet to be clarified. Finally, it is the oldest and most robust technique (first publications in the 90s) and the most widely used, mainly in the field of tumors [105-111]. In this, DCE-MRI is the functional magnetic resonance imaging (f-MRI) technique unanimously recognized as the gold standard in the evaluation of organ perfusion [12, 61, 62, 112, 113] and we demonstrate that, despite current limitation related to uncertainty about contrast agent safety in human pregnancies, as a technique it is also relevant for studying placental function.

Other functional MRI techniques may also be able to assess placental function, but not as accurately and extensively as DCE-MRI could allow. ASL-MRI (Arterial Spin Labeling), uses MRI pulses to magnetically label blood as an endogenous contrast agent [114]. Studies have shown its feasibility for the quantification of placental perfusion in rats [115] and humans [116-117]. Although its main strength is the absence of contrast agent injected, ASL-MRI is nonetheless limited ~~by the poor signal to noise ratio and~~ its high sensitivity to motion artifacts [61, 118]. Often criticized for its low SNR, Harteveld nevertheless emphasizes that a high SNR can be obtained on the condition of using low cutoff velocity (1.6cm/s) [119]. Other non-contrast techniques, DWI (diffusion weighted imaging) and IVIM (intravoxel incoherent Motion) are techniques that also makes it possible to assess perfusion parameters: ADC (apparent diffusion coefficient) and perfusion fraction (f, %) by studying the movement and diffusion of water molecules within tissues [120]. The exact nature of what is measured with placental IVIM remains controversial [62]. Derwig et al have compared IVIM and ASL in the assessment of placental perfusion in the second trimester in normal and fetal growth restriction pregnancies and suggest that the FAIR-ASL sequence may offer a more practically suitable method for routine clinical application than IVIM [121].

The future of DCE-MRI undoubtedly lies in the widespread availability of safe contrast agents, be they Gd based or other. They make it possible to overcome several limitations of the DCE-MRI which have hindered its development until now. Animal studies have shown that some newer agents do not cross the placenta, suggesting that they might be safe if they cannot reach the fetus. However, studies in humans are still lacking at present on this subject. Remaining in the intervillous space, they make it possible to overcome the

complexity of compartmental analysis while retaining the potential to study the maternal portion - the inter-villous space of the placenta, involved in the pathophysiological process of placental insufficiency.

Conclusion

DCE-MRI is the oldest and most robust method for assessing organ function as a whole (perfusion and permeability). This depth and breadth make it to this day as a gold-standard technique in studying perfusion. While its use in the human placenta has been hampered by the need for gadolinium based-contrast agents whose safety remains controversial, the recent development of novel contrast agents such as liposomal-gadolinium and SPIO, two contrast agents that do not cross the placenta barrier, now introduce new avenues for further exploration. In addition, with the increasing development of other f-MRI techniques, exciting perspectives can be envisaged such as their combination with each other, or wider application of such techniques in fetal interventions such as in monochorionic twin pregnancies.

Funding: This research did not receive any specific grant from funding agencies in the public, commercial, or not-for-profit sectors.

References:

[1] Romero R, Kusanovic JP, Kim CJ. Placental bed disorders in the genesis of the great obstetrical syndromes. In: Pijnenborg R, Brosens I, Romero R, eds. Placental bed disorders. Basic science and its translation to obstetrics. Cambridge, UK: Cambridge University Press; 2010:271-89.

[2] Brosens I, Pijnenborg R, Vercruysse L, RomeroR. The "great obstetrical syndromes" are associated with disorders of deep placentation. Am J Obstet Gynecol 2011;204:193-201.

[3] Baschat AA, Hecher K. Fetal growth restriction due to placental disease. Semin Perinatol 2004;28:67-80.

[4] Audus KL. Controlling drug delivery across the placenta. Eur J Pharm Sci 1999;8:161–165.

[5] Garland M. Pharmacology of drug transfer across the placenta. Obstet Gynecol Clin North Am 1998;25:21–42.

[6] Olsen GD. Placental permeability for drugs of abuse and their metabolites. NIDA Res Monogr 1995;154:152–162.

[7] Maidji E, Percivalle E, Gerna G, Fisher S, Pereira L. Transmission of human cytomegalovirus from infected uterine microvascular endothelial cells to differentiating/invasive placental cytotrophoblasts. Virology 2002;304:53–69.

[8] Brix G, Schreiber W, Hoffmann U, et al. Methodological approaches to quantitative evaluation of microcirculation in tissues with dynamic magnetic resonance tomography.Radiologe 1997;37:470-80.

[9] Yankeelov TE, Gore JC. Dynamic Contrast Enhanced Magnetic Resonance Imaging in Oncology: Theory, Data Acquisition, Analysis, and Examples. Curr Med Imaging Rev 2009;3:91-107.

[10] Brix G, Kiessling F, Lucht R, et al. Microcirculation and microvasculature in breast tumors: pharmacokinetic analysis of dynamic MR image series. Magn Reson Med 2004;52:420-9.

[11] Cuenod, C.A.; Balvay, D. (2013). Perfusion and vascular permeability: Basic concepts and measurement in DCE-CT and DCE-MRI. Diagnostic and Interventional Imaging, 94(12), 1187–1204.

[12] O'Connor, J P B; Tofts, P S; Miles, K A; Parkes, L M; Thompson, G; Jackson, A (2011). Dynamic contrast-enhanced imaging techniques: CT and MRI. The British Journal of Radiology, 84(special_issue_2), S112–S120.

[13] Li X, Huang W, Rooney WD. Signal-to-noise ratio, contrast-to-noise ratio and pharmacokinetic modeling considerations in dynamic contrast-enhanced magnetic resonance imaging. Magnetic Resonance Imaging 30 (2012) 1313–1322

[14] Schabel MC, Parker DL. Uncertainty and bias in contrast concentration measurements using spoiled gradient echo pulse sequences. Phys Med Biol. 2008 May 7; 53(9): 2345–2373.

[15] De Naeyer D, Verhulst J, Ceelen W, Segers P, De Deene Y, Verdonck P. Flip angle optimization for dynamic contrast-enhanced MRI-studies with spoiled gradient echo pulse sequences. Phys. Med. Biol. 56 (2011) 5373–5395

[16] Zhang JL, Koh TS. On the Selection of Optimal Flip Angles for Mapping of Breast Tumors with Dynamic Contrast-Enhanced Magnetic Resonance Imaging. IEEE TRANSACTIONS ON BIOMEDICAL ENGINEERING, VOL. 53, NO. 6, JUNE 2006

[17] Xiao, Yu-Dong; Paudel, Ramchandra; Liu, Jun; Ma, Cong; Zhang, Zi-Shu; Zhou, Shun-Ke (2016). MRI contrast agents: Classification and application (Review). International Journal of Molecular Medicine

[18] Webb, J.A., H.S. Thomsen, and S.K. Morcos, The use of iodinated and gadolinium contrast media during pregnancy and lactation. Eur Radiol, 2005. 15(6): p. 1234-40.

[19] Lin, S.P. and J.J. Brown, MR contrast agents: physical and pharmacologic basics. J Magn Reson Imaging, 2007. 25(5): p. 884-99.

[20] Palacios Jaraquemada, J.M. and C. Bruno, Gadolinium-enhanced MR imaging in the differential diagnosis of placenta accreta and placenta percreta. Radiology, 2000. 216(2): p. 610-1.

[21] Prola-Netto J, Woods M, Roberts VHJ, Sullivan EL, Miller CA, Frias AE, Oh KY. Gadolinium Chelate Safety in Pregnancy: Barely Detectable Gadolinium Levels in the Juvenile Nonhuman Primate after in Utero Exposure. Radiology. 2018 Jan;286(1):122-128

[22] Ray JG, Vermeulen MJ, Bharatha A, Montanera WJ, Park AL. Association between MRI exposure during pregnancy and fetal and childhood outcomes. JAMA 2016;316:952–961.

[23] De Santis M, Straface G, Cavaliere AF, Carducci B, Caruso A. Gadolinium periconceptional exposure: pregnancy and neonatal outcome. Acta Obstet Gynecol Scand 2007;86:99–101.

[24] Fraum, T. J., Ludwig, D. R., Bashir, M. R. & Fowler, K. J. Gadolinium-based contrast agents: A comprehensive risk assessment. J. Magn. Reson. Imaging 46, 338–353 (2017).

[25] Gale EM, Atanasova IP, Blasi F, Ay I, Caravan P. A Manganese Alternative to Gadolinium for MRI Contrast, J. Am. Chem. Soc. (2015).

[26] Ishida O, Maruyama K, Sasaki K, Iwatsuru M (1999) Size-dependent extravasation and interstitial localization of polyethyleneglycol liposomes in solid tumor-bearing mice. Int J Pharm 190: 49–56.

[27] Gabizon A, Shmeeda H, Barenholz Y (2003) Pharmacokinetics of pegylated liposomal Doxorubicin: review of animal and human studies. Clin Pharmacokinet 42: 419–36.

[28] Ayyagari AL, Zhang X, Ghaghada KB, Annapragada A, Hu X, et al. (2006) Long-circulating liposomal contrast agents for magnetic resonance imaging. Magn Reson Med 55: 1023–9.

[29] Ghaghada, K., Hawley, C., Kawaji, K., Annapragada, A. & Mukundan, S. T1 relaxivity of core-encapsulated gadolinium liposomal contrast agents–effect of liposome size and internal gadolinium concentration. Acad Radiol 15, 1259–1263 (2008).

[30] Tilcock C, MacDougall P, Unger E, et al. The effect of lipid composition on the relaxivity of Gd-DTPA entrapped in lipid vesicles of defined size. Biochim Biophys Acta 1990; 1022:181–186.

[31] Fossheim SL, Fahlvik AK, Klaveness J, et al. Paramagnetic liposomes as MRI contrast agents: influence of liposomal physicochemical properties on the in vitro relaxivity. Magn Reson Imaging 1999; 17:83–89.

[32] Ghaghada KB, Ravoori M, Sabapathy D, Bankson J, Kundra V, et al. (2009) New Dual Mode Gadolinium Nanoparticle Contrast Agent for Magnetic Resonance Imaging. PLoS ONE 4(10): e7628. doi:10.1371/journal.pone.0007628

[33] Ayyagari AL, Zhang X, Ghaghada KB, Annapragada A,Hu X, Bellamkonda RV. Long-circulating liposomal contrast agents for magnetic resonance imaging. (2006), 55(5), 1023–1029.

[34] Shetty AN, Pautler R, Ghaghada K, Rendon D, Gao H, Starosolski Z, Bhavane R, Patel C, Annapragada A, Yallampalli C, Lee W. A liposomal Gd contrast agent does not cross the mouse placental barrier, Sci Rep. 6 (2016) 27863.

[35] Ghaghada KB, Starosolski ZA, Bhayana S, Stupin I, Patel CV, Bhavane RC, Gao H, Bednov A, Yallampalli C, Belfort M, George V, Annapragada AV. Pre-clinical evaluation of a nanoparticle-based blood-pool contrast agent for MR imaging of the placenta. Placenta. 2017 Sep; 57:60-70.

[36] Badachhape AA, Devkota L, Stupin IV, Sarkar P, Srivastava M, Tanifum EA, Fox KA, Yllampalli C, Annapragada AV, Ghaghada KB. Nanoparticle Contrast-enhanced T1-Mapping Enables Estimation of Placental Fractional Blood Volume in a Pregnant Mouse Model. Sci Rep. 2019 Dec 10;9(1):18707.

[37] Reimer P, Balzer T (2003). *Ferucarbotran (Resovist): a new clinically approved RES-specific contrast agent for contrast-enhanced MRI of the liver: properties, clinical development, and applications. , 13(6), 1266–1276.* doi:10.1007/s00330-002-1721-7

[38] Toth GB, Varallyay CG, Horvath A, Bashir MR, Choyke PL, Daldrup-Link HE and al. Current and potential imaging applications of ferumoxytol for magnetic resonance imaging. Kidney Int 2017;92(1):47–66.

[39] Zhu A, Reeder SB, Johnson KM, Nguyen SM, Fain SB, Bird IM, Golos TG, Wieben O, Shah DM, Hernando D. Quantitative ferumoxytol-enhanced MRI in pregnancy: A feasibility study in the nonhuman primate. Magn Reson Imaging. 2020 Jan; 65:100-108.

[40] Nguyen SM, Wiepz GJ, Schotzko M, Simmons HA, Mejia A, Ludwig KD, Zhu A, Brunner K, Hernando D, Reeder SB, Wieben O, Johnson K, Shah D, Golos TG. Impact of ferumoxytol magnetic resonance imaging on the rhesus macaque maternal-fetal interface†. Biol Reprod. 2020 Feb 14;102(2):434-444.

[41] Deloison B, Siauve N, Aimot S, Balvay D, Thiam R, Cuenod C, Ville Y, Clement O, Salomon LJ. SPIO-enhanced magnetic resonance imaging study of placental perfusion in a rat model of intrauterine growth restriction: Placental perfusion in MRI, BJOG: An International Journal of Obstetrics & Gynaecology. 119 (2012) 626–633.

[42] Schnall MD, Blume J, Bluemke DA.; DeAngelis GA, DeBruhl n, Harms S, Heywang-Köbrunner SH.; Hylton N, Kuhl CK, Pisano ED, Causer P, Schnitt, SJ, Thickman D, Stelling CB, Weatherall PT, Lehman C, Gatsonis, CA. (2006). Diagnostic Architectural and Dynamic Features at Breast MR Imaging: Multicenter Study. Radiology, 238(1), 42–53.

[43] Lavini C, de Jonge MC, van de Sande MG, et al. Pixel-by-pixel analysis of DCE MRI curve patterns and an illustration of its application to the imaging of the musculoskeletal system. Magn Reson Imaging 2007;25:604-12.

[44] Galbraith SM, Lodge MA, Taylor NJ, et al. Reproducibility of dynamic contrast-enhanced MRI in human muscle and tumours: comparison of quantitative and semi-quantitative analysis. NMR Biomed 2002;15:132-42.

[45] Walker-Samuel S, Leach MO, Collins DJ. Evaluation of response to treatment using DCE-MRI: the relationship between initial area under the gadolinium curve (IAUGC) and quantitative pharmacokinetic analysis. Phys Med Biol 2006;51:3593-602.

[46] Medved M, Karczmar G, Yang C, Dignam J, Gajewski TF, Kindler H, et al. Semiquantitative analysis of dynamic contrast enhanced MRI in scancer patients: variability and changes in tumor tissue over time. J Magn Reson Imaging 2004;20:122– 8.

[47] Fritz-Hansen T, Rostrup E, Larsson HBW, Sondergaard L, Ring P, Henrikson O. Measurement of the arterial concentration of Gd-DTPA using MRI: a step toward quantitative perfusion imaging. Magn Reson Med 1996;36:225– 31.

[48] Larsson HBW, Stubgaard M, Frederiksen JL, Jensen M, Henriksen O, Paulson OB. Quantitation of blood–brain barrier defect by magnetic resonance imaging and gadolinium-DTPA in patients with multiple sclerosis and brain tumors. Magn Reson Med 1990;16:117–31.

[49] Weinmann H-J, Laniado M, Mu¨ tzel W. Pharmacokinetics of GdDTPA/dimeglumine after intravenous injection into healthy volunteers. Physiol Chem Phys Med NMR 1984;16:167–172.

[50] Parker GJM. Monitoring contrast agent kinetics using dynamic MRI: quantitative and qualitative analysis. Ph.D. dissertation, University of London, London, UK, 1997.

[51] Parker GJM, Tanner SF, Leach MO. Pitfalls in the measurement of tissue permeability over short time-scales using multi-compartment models with a low temporal resolution blood input function. In: Proceedings of the 4th Annual Meeting of ISMRM, New York, NY, USA,1996. p 1582.

[52] Parker GJM, Roberts C, Macdonald A, Buonaccorsi GA, Cheung S, Buckley DL, Jackson A, Watson Y, Davies K, Jayson GC. Experimentally-derived functional form for a population-averaged high-temporal-resolution arterial input function for dynamic contrast-enhanced MRI, Magn. Reson. Med. (2006)

[53] Yankeelov TE, Luci JJ, Lepage M, Li R, Debusk L, Lin PC, Price RR, Gore JC. Quantitative pharmacokinetic analysis of DCE-MRI data without an arterial input function: A reference region model, Magn. Reson. Imaging. (2005).

[54] Enders AC, Blankenship TN. Comparative placental structure. Adv Drug Deliv Rev 1999;38:3–15.

[55] Georgiades, P., Ferguson-Smith, A. and Burton, G. (2002) Comparative development anatomy of the murine and human definitive placentae. Placenta, 23, 3±19.

[56] Roberts VHJ, Rasanen JP, Novy MJ, Frias A, Louey S, Morgan TK, Thornburg KL, Spindel ER, Grigsby PL. Restriction of placental vasculature in a non-human primate: a unique model to study placental plasticity. Placenta 2012;33:73–76

[57] Malassiné A, Frendo JL, Evain-Brion D. A comparison of placental development and endocrine functions between the human and mouse model. Human Reproduction Update, Vol.9, No.6 pp. 531±539, 2003

[58] Furukawa S, Tsuji N, Sugiyama A. Morphology and physiology of rat placenta for toxicological evaluation. J Toxicol Pathol 2019; 32: 1–17

[59] Brix G, Semmler W, Port R, et al. Pharmacokinetic parameters in CNS Gd-DTPA enhanced MR imaging. J Comput Assist Tomogr 1991;15:621-8.10.

[60] Tofts PS, Kermode AG. Measurement of the blood-brain barrier permeability and leakage space using dynamic MR imaging. 1. Fundamental concepts. Magn Reson Med 1991;17:357-67.

[61] Siauve N, Chalouhi GE, Deloison B, Alison M, Clement O, Ville Y, Salomon LJ. Functional imaging of the human placenta with magnetic resonance. Am J Obstet Gynecol. 2015 Oct;213(4 Suppl):S103-14.

[62] Chalouhi G.E, Deloison B, Siauve N, Aimot S, Balvay D, Cuenod CA, Ville Y, Clément O, Salomon LJ. Dynamic contrast-enhanced magnetic resonance imaging: Definitive imaging of placental function? Semin Fetal Neonatal Med. 2011 Feb;16(1):22-8. doi: 10.1016/j.siny.2010.09.001. Epub 2010 Sep 20. PMID: 20851065.

[63] K.A. Miles. Measurement of tissue perfusion by dynamic computed tomography. Br J Radiol 1991 May;64(761):409e12.

[64] Schabel MC. A unified impulse response model for DCE-MRI. Magn Reson Med. 2012; 68:1632–1646

[65] Frias AE, Schabel MC, Roberts VHJ, et al. Using dynamic contrast-enhanced MRI to quantitatively characterize maternal vascular organization in the primate placenta. Magn Reson Med 2015; 73:1570-8.

[66] Salomon LJ, Siauve N, Balvay D, Cuénod CA, Vayssettes C, Luciani A, Frija G, Ville Y, Clément O. Placental Perfusion MR Imaging with Contrast Agents in a Mouse Model, Radiology. 235 (2005) 73–80.

[67] Taillieu F, Salomon LJ, Siauve N, Clément O, Faye N, Balvay D, Vayssettes C, Frija G, Ville Y, Cuenod CA. Placental Perfusion and Permeability: Simultaneous Assessment with Dual-Echo Contrast-342 enhanced MR Imaging in Mice, Radiology. 241 (2006) 737–745.

[68] Alison M, Quibel T, Balvay D, Autret G, Bourillon C, Chalouhi GE, Deloison B, Brix G, Bahner ML, Hoffmann U, Horvath A, Schreiber W (1999). Regional Blood Flow, Capillary Permeability, and Compartmental Volumes: Measurement with Dynamic CT—Initial Experience. doi:10.1148/radiology.210.1.r99ja46269

[69] Remus CC, Sedlacik J, Wedegaertner U, Arck P, Hecher K, Adam G, Forkert ND. Application of the steepest slope model reveals different perfusion territories within the mouse placenta, Placenta, 11 Jul 2013, 34(10):899-906.

[70] Yadav BK, et al., A longitudinal study of placental perfusion using dynamic contrast enhanced magnetic resonance imaging in murine pregnancy, Placenta (2016), http://dx.doi.org/10.1016/j.placenta.2015.12.019

[71] Salomon LJ, Siauve N, Taillieu F and al. In Vivo Dynamic MRI Measurement of the Noradrenaline-induced Reduction in Placental Blood Flow in Mice, Placenta. 27 (2006) 1007–1013.

[72] Lémery Magnin M, Fitoussi V, Siauve N, Pidial L, Balvay D, Autret G, Cuenod CA, Clément O, Salomon LJ. Assessment of Placental Perfusion in the Preeclampsia L-NAME Rat Model with High-Field Dynamic Contrast-Enhanced MRI, Fetal Diagnosis and Therapy. (2018) 1–8.

[73] Drobyshevsky A, Prasad PV. Placental perfusion in uterine ischemia model as evaluated by dynamic contrast enhanced MRI. J Magn Reson Imaging. 2015 Sep;42(3):666-72.

[74] Remus CC, Solano E, Ernst T, Thieme R, Hecher K, Adam G, Arck P. Comparative analysis of high field MRI and histology for ex vivo whole organ imaging: assessment of placental functional morphology in a murine model. MAGMA. 2019 Apr;32(2):197-204.

[75]Arthuis CJ,Mendes V, Même S, Même W, Rousselot R, Winer N, Novell A, Perrotin F. Comparative determination of placental perfusion by magnetic resonance imaging and contrast-enhanced ultrasound in a murine model of intrauterine growth restriction. Placenta. 2018 Sep;69:74-81.

[76] Couper S, Clark A, Thompson JMD, Flouri D, Aughwane R, David AL, Melbourne A, Mirjalili A, Stone PR. The effects of maternal position, in late gestation pregnancy, on placental blood flow and oxygenation: an MRI study, J. Physiol. (2020).

[77] Adamson SL, Lu Y, Whiteley KJ, Holmyard D, Hemberger M, Pfarrer C, et al. Interactions between trophoblast cells and the maternal and fetal circulation in the mouse placenta, Dev. Biol. 250 (2002) 358e373, https://doi.org/10.1006/dbio.2002.0773.

[78] Solano ME, Kowal MK, O'Rourke GE, Horst AK, Modest K, Plosch T, et al. Progesterone and HMOX-1 promote fetal growth by CD8. T cell modulation, J. Clin. Invest. 125 (2015) 1726e1738

[79] Tarrade A, Lecarpentier E, Gil S, Morel O, Zahr N, Dahirel M, et al: Analysis of placental vascularization in a pharmacological rabbit model of IUGR induced by L-NAME, a nitric oxide synthase inhibitor. Placenta 2014;35:254-259

[80] de Bazelaire C, Siauve N, Fournier L, Frouin F, Vernoux S, Kahn E, Clement O, Frija G, Cuenod CA. Comprehensive model for simultaneous perfusion and permeability MRI. Magn Reson Med (Submitted Aug. 02).

[81] Tofts PS, Kermode AG. Blood-brain barrier permeability in multiple sclerosis using labelled STPA with PET, CT and MRI. J Neurol Neurosurg Psychiatry 1959; 52:1019-20;

[82] Larsson HB, Fritz-Hansen T, Rostrup E, Sondergaard L, Ring P, Henriksen O. Myocardial perfusion modeling using MRI. MagnReson Med 1996;35:716-26

[83] Pradel C, Siauve N, Bruneteau G, Clement O, de Bazelaire C, Frouin F, Wedge SR, Tessier JL, Robert PH, Frija G, Cuenod CA (2003) Reduced capillary perfusion and permeability in human tumour xenografts treated with the VEGF signalling inhibitor ZD4190: an in vivo assessment using dynamic MR imaging and macromolecular contrast media. Magn Reson Imaging 21:845–851

[84] Millischer AE, Salomon LJ, Porcher R, Brasseur-Daudruy M, Gourdier AL, Hornoy P, Silvera S, Loisel D, Tsatsaris V, Delorme B, Boddaert N, Ville Y, Sentilhes L. Magnetic resonance imaging for abnormally invasive placenta: the added value of intravenous gadolinium injection, BJOG: An International Journal of Obstetrics & Gynaecology. 124 (2017) 88–95.

[85] C.R. Warshak, R. Eskander, A.D. Hull, A.L. Scioscia, R.F. Mattrey, K. Benirschke, R. Resnik, Accuracy of Ultrasonography and Magnetic Resonance Imaging in the Diagnosis of Placenta Accreta:, Obstetrics & Gynecology. 108 (2006) 573–581.

[86] H.B. Marcos, R.C. Semelka, S. Worawattanakul, Normal placenta: gadolinium-enhanced dynamic MR imaging., Radiology. 205 (1997) 493–496.

[87] R. Brunelli, G. Masselli, T. Parasassi, M. De Spirito, M. Papi, G. Perrone, E. Pittaluga, G. Gualdi, E. Pollettini, A. Pittalis, M.M. Anceschi, Intervillous circulation in intra17 uterine growth restriction. Correlation to fetal wellbeing, Placenta. 31 (2010) 1051–1056.

[88] V. Romeo, L. Sarno, A. Volpe, M.I. Ginocchio, R. Esposito, P.P. Mainenti, M. Petretta, R. Liuzzi, M. D'Armiento, P. Martinelli, A. Brunetti, S. Maurea, US and MR imaging findings to detect placental adhesion spectrum (PAS) in patients with placenta previa: a comparative systematic study, Abdom Radiol (NY). 2019 Oct;44(10):3398-3407.

[89] H. Kapoor, M. Hanaoka, A. Dawkins, A. Khurana, Review of MRI imaging for placenta accreta spectrum: Pathophysiologic insights, imaging signs, and recent developments, Placenta. (2021).

[90] A. Kilcoyne, A.S. Shenoy-Bhangle, D.J. Roberts, R.C. Sisodia, D.A. Gervais, S.I. Lee, MRI of placenta accreta, placenta increta, and placenta percreta: pearls and pitfalls, Am. J. Roentgenol. 208 (2017) 214–221.

[91] A.A. Zaghal, H.K. Hussain, G.A. Berjawi, MRI evaluation of the placenta from normal variants to abnormalities of implantation and malignancies, J. Magn. Reson. Imag. 50 (2019) 1702–1717.

[92] PJ Woodward, A. Kennedy, B.D. Einerson, Is there a role for MRI in the management of placenta accreta spectrum? Curr. Obstet. Gynecol. Rep. 8 (2019) 64–70.

[93] E. Jauniaux, A. Bhide, A. Kennedy, P. Woodward, C. Hubinont, S. Collins, et al., FIGO consensus guidelines on placenta accreta spectrum disorders: prenatal diagnosis and screening, Int. J. Gynecol. Obstet. 140 (2018) 274–280.

[94] J.M. Palacios-Jaraquemada, C.H. Bruno, E. Martín, MRI in the diagnosis and surgical management of abnormal placentation, Acta Obstet. Gynecol. Scand. 92 (2013) 392–397.

[95] F. D'Antonio, C. Iacovella, J. Palacios-Jaraquemada, C.H. Bruno, L. Manzoli, A. Bhide, Prenatal identification of invasive placentation using magnetic resonance imaging: systematic review and meta-analysis, Ultrasound Obstet. Gynecol. 44 (2014) 8–16.

[96] X. Meng, L. Xie, W. Song, Comparing the diagnostic value of ultrasound and magnetic resonance imaging for placenta accreta: a systematic review and meta-analysis, Ultrasound Med. Biol. 39 (2013) 1958–1965.

[97] A. Lax, M.R. Prince, K.W. Mennitt, J.R. Schwebach, N.E. Budorick, The value of specific MRI features in the evaluation of suspected placental invasion, Magn. Reson. Imaging 25 (2007) 87–93.

[98] Y. Ueno, T. Maeda, U. Tanaka, K. Tanimura, K. Kitajima, Y. Suenaga, et al., Evaluation of interobserver variability and diagnostic performance of developed MRI-based radiological scoring system for invasive placenta previa, J. Magn. Reson. Imag. 44 (2016) 573–583.

[99] A. Familiari, M. Liberati, P. Lim, G. Pagani, G. Cali, D. Buca, et al., Diagnostic accuracy of magnetic resonance imaging in detecting the severity of abnormal invasive placenta: a systematic review and meta-analysis, Acta Obstet. Gynecol. Scand. 97 (2018) 507–520.

[100] S.L. Collins, A. Ashcroft, T. Braun, P. Calda, J. Langhoff-Roos, O. Morel, et al., Proposal for standardized ultrasound descriptors of abnormally invasive placenta (AIP), Ultrasound Obstet. Gynecol. 47 (2016) 271–275.

[101] P. Jha, L. P¯oder, C. Bourgioti, N. Bharwani, S. Lewis, A. Kamath, et al., Society of Abdominal Radiology (SAR) and European Society of Urogenital Radiology (ESUR) joint consensus statement for MR imaging of placenta accreta spectrum disorders, Eur. Radiol. 30 (2020) 2604–2615.

[102] Benchimol G, Deloison B, Balvay1 D, Bussieres L, Millischer L, Grevent D, Butor C, Chalouhi GE, Mahallati H, Ville Y, Siauve N, Salomon LJ. Reference ranges for placental perfusion using dynamic contrast enhancement magnetic resonance imaging, OC28.01
29th World Congress on Ultrasound in Obstetrics and Gynecology, doi:10.1002/uog.20618

[103] J. Bodis, K. Zambo, Z. Nemessanyi, E. Mate, ImreF. Csaba, Application of the parametric scan in the investigation of uteroplacental blood flow, European Journal of Nuclear Medicine. 10–10 (1985).

[104] Gowland PA, Francis ST, Duncan KR, Freeman AJ, Issa B, Moore RJ, Bowtell RW, Baker PN, Johnson IR, Worthington BS. In vivo perfusion measurements in the human placenta using echo planar imaging at 0.5 T. 1998. Magnetic Resonance Imaging, 40(3), 467–473

[105] A.R. Padhani, A.A Khan, Diffusion-weighted (DW) and dynamic contrast-enhanced (DCE) magnetic resonance imaging (MRI) for monitoring anticancer therapy**.** Targ Oncol (2010) 5:39–52

[106] I. Thomassin-Naggara, M. Bazot, E. Daraï, P. Callard, J. Thomassin, C.A. Cuenod and al, Epithelial ovarian tumors: value of dynamic contrast-enhanced MR imaging and correlation with tumor angiogenesis. Radiology, 2008. 248(1): p. 148-59.

[107] J.L. Evelhoch, Key Factors in the Acquisition of Contrast Kinetic Data for Oncology, Journal of Magnetic Resonance Imaging (1999) 10:254–259

[108] E. Henderson, K.E. Rutt, T.Y. Lee, Temporal sampling requirements for the tracer kinetics modeling of breast disease, Magnetic Resonance Imaging, Vol. 16, No. 9, pp. 1057–1073, 1998

[109] Soheil L. Hanna; Wilburn E. Reddick; David M. Parham; Suzanne A. Gronemeyer; June S. Taylor; Barry D. Fletcher (1993). Automated pixel-by-pixel mapping of dynamic contrast-enhanced MR images for evaluation of osteosarcoma response to chemotherapy: Preliminary results. , 3(6), 849–853. doi:10.1002/jmri.1880030609

[110] Jeffrey L. Evelhoch (1999). Key factors in the acquisition of contrast kinetic data for oncology. , 10(3), 254–259. doi:10.1002/(sici)1522-2586(199909)10:3<254::aid-jmri5>3.0.co;2-9

[111] Jackson A, O'Connor J, Thompson G, Mills S. Magnetic resonance perfusion imaging in neuro-oncology. Cancer Imaging 2008;8:186–99.

[112] Sourbron S. Technical aspects of MR perfusion. Eur J Radiol 2010;76:304-13.

[113] Guttmacher AE, Maddox YT, Spong CY. The Human Placenta Project: placental structure, development, and function in real time. Placenta 2014;35:303-4.

[114] Wong EC. An introduction to ASL labeling techniques. J Magn Reson Imaging 2014;40: 1-10.

[115] Deloison B, Salomon LJ, Quibel T, Chalouhi GE, Alison M, Balvay D, Autret G, Cuenod CA, Clement O, Siauve N. Non-invasive assessment of placental perfusion in vivo using arterial spin labeling (ASL) MRI: A preclinical study in rats. Placenta 77 (2019) 39–45

[116] Liu D, Shao X, Danyalov A, Chanlaw T, Masamed R, Wang DJJ, Janzen C, Devaskar SU, Sung K. Human Placenta Blood Flow During EarlyGestation With Pseudocontinuous Arterial Spin Labeling MRI. J. MAGN. RESON. IMAGING 2019. DOI: 10.1002/jmri.26944

[117] Zun Z, Limperopoulos C. Placental Perfusion Imaging Using Velocity-Selective Arterial Spin Labeling. Magn Reson Med. 2018 September; 80(3):1036-1047

[118] Aughwane R, Ingram E, Johnstone ED, Salomon LJ, David AL, Melbourne A. Placental MRI and its application to fetal intervention. Prenatal Diagnosis. 2020;40:38–48.

[119] Harteveld AA, Hutter J, Franklin SL, Jackson LH, Rutherford M, Hajnal JV, De Vita E. Systematic evaluation of velocity-selective arterial spin labeling settings for placental perfusion measurement. Magnetic Resonance in Medicine. 2020 Oct;84(4):1828-1843

[120] Le Bihan D. Diffusion, confusion and functional MRI. Neuroimage 2012;62:1131-6.

[121] Derwig I, et al., Association of placental perfusion, as assessed by magnetic resonance imaging and uterine artery Doppler ultrasound, and its relationship to pregnancy outcome, Placenta (2013), http://dx.doi.org/10.1016/j.placenta.2013.07.006

Figure Legends

Figure 1: Example of dynamic contrast-enhanced magnetic resonance imaging of human placenta: A, After arrival of a bolus of intravenous injection of contrast media the aorta (red arrow) enhances; while the unenhanced placenta appears as low signal on T1-weighted sequences (blue outline). B-C, Shortly after the intravenous injection of gadolinium chelate in the arteries, the placenta enhances gradually and shows high signal on T1W images. After compartmental analysis of the enhancement, functional parameters can be evaluated.

Figure 2: The placental tissue enhancement curve
FT: Tissue blood flow, Vb: Tissue blood volume, PS: surface area product, Ve: Tissue interstitial volume.

Figure 3: Three-compartment model of the placenta. Exchanges of contrast media between the compartments are governed by transfer constants (k). q: quantity of contrast medium

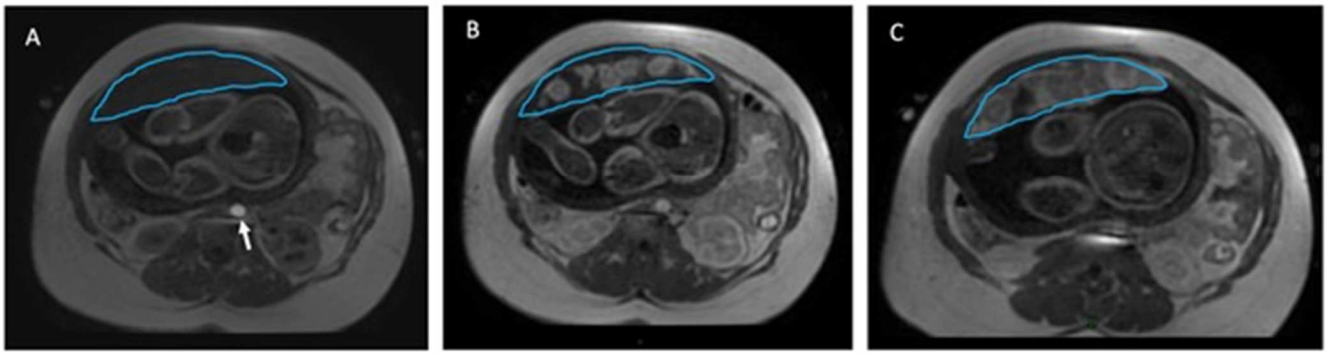

Figure 1

Figure 2

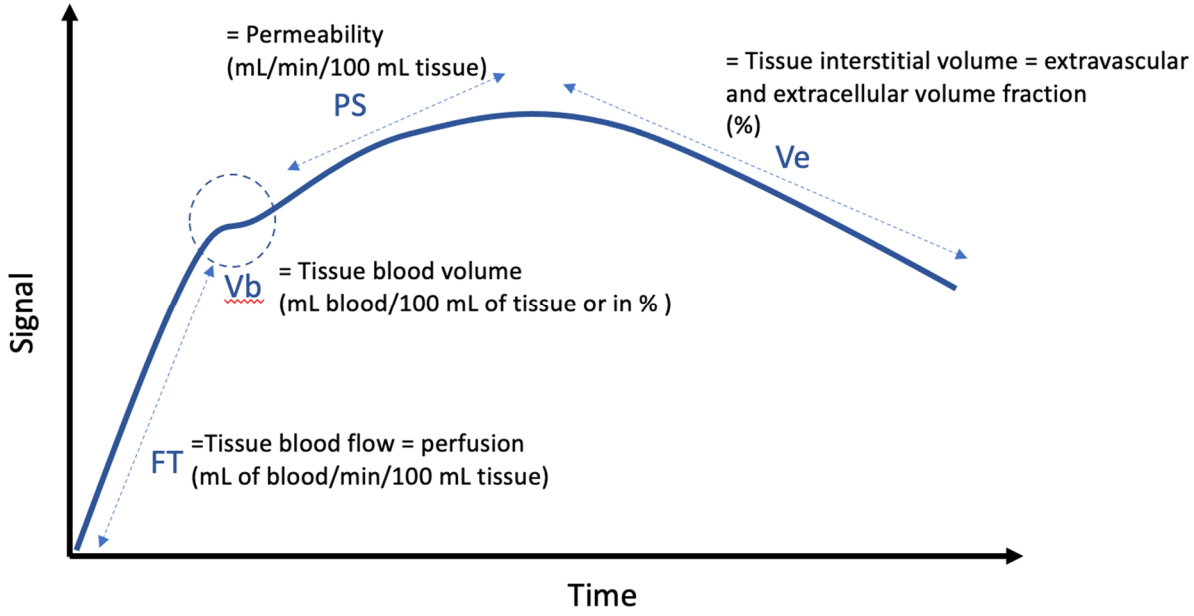
= Permeability
(mL/min/100 mL tissue)
PS
= Tissue interstitial volume = extravascular and extracellular volume fraction
(%)
Ve
Vb
= Tissue blood volume
(mL blood/100 mL of tissue or in %)
FT
=Tissue blood flow = perfusion
(mL of blood/min/100 mL tissue)
Signal
Time

Figure 3

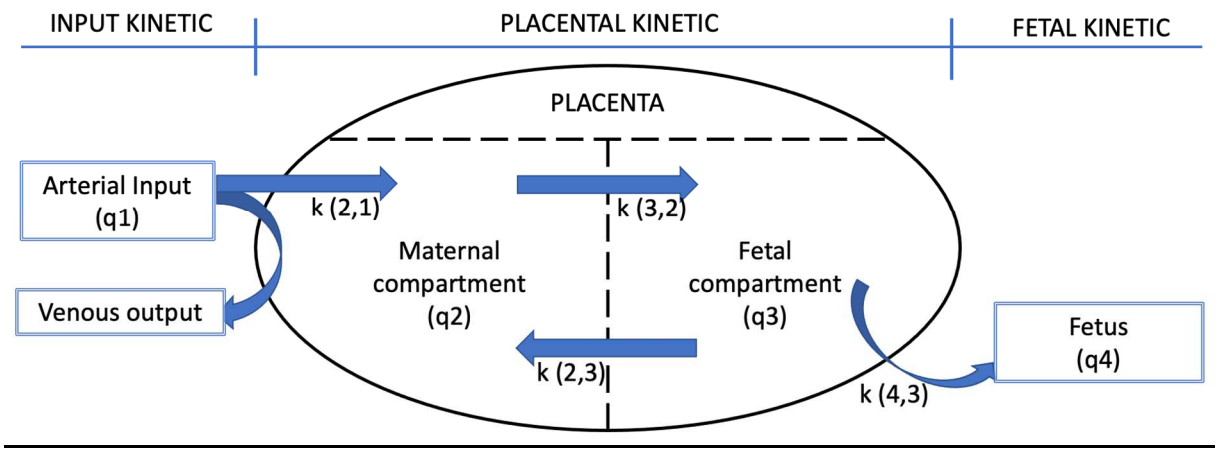
INPUT KINETIC
PLACENTAL KINETIC
FETAL KINETIC
PLACENTA
Arterial Input
(q1)
Venous output
k (2,1)
k (3,2)
Maternal
compartment
(q2)
Fetal
compartment
(q3)
k (2,3)
k (4,3)
Fetus
(q4)

Table 1:
Title: Results of animal placental perfusion imaging studies in normal physiological conditions.
Caption: F: placental blood flow, Vb: fractional volume of the maternal vascular placental compartment, ED: embryonic day, Gd-CA: Gadolinium-based contrast agent, Gd: Gadolinium, T: Tesla, N/A: not applicable, 2D/3D: two/three-dimensional, HPZ: high perfusion zone, LPZ: low perfusion zone. NB: the length of pregnancy for mice is 19 days and 165 days for rhesus monkeys. All the EDs mentioned in the studies below therefore correspond to a period roughly similar to the third trimester in humans.

Table 2:
Title: Results of animal placental perfusion imaging studies in pathological conditions
Statistically significant results are denoted with an asterisk *

Table 3:
Title: Main characteristics of the three-compartment pharmacokinetic model compared to the steepest-slope model. AIF: Arterial Input Function

Table 4:
Title: Mains characteristics of Gd-CA, liposomal-Gd and SPIO contrast agents

ARTICLE	POPULA-TION	CONTRAST AGENT	IMAGING SEQUENCE	TYPE OF ANALYSIS	F ($ML*MIN^{-1}*100ML^{-1}$) MEAN ± SD	VB (%)
SALOMON ET AL 2005[66]	36 mice (ED16)	Gd-CA	1.5T 2D fast spoiled gradient-echo sequence	Three compartmental model	128+60	N/A
TAILLIEU ET AL 2006 [67]	22 Mice (ED16)	Gd-CA	1.5T 2D fast spoiled gradient-echo single slice sequence with a dual echo time	Three compartmental model	180	36.5±0.9
REMUS ET AL 2013 [69]	5 mice (ED14.5) 5 mice (ED16.5)	Gd-CA	7 T 3D T1-weighted gradient-echo sequence	Steepest slope model	Whole placenta ED14.5: 135±29 ED16.5: 112±32 HPZ: ED14.5: 184±39 ED16.5: 158±58 LPZ: ED14.5: 119±28 ED16.5: 114±52	N/A
YADAV ET AL 2015 [70]	7 mice (ED13,15,17)	Gd-CA	7 T multi-slice 2D spoiled gradient echo sequence	Steepest slope model	Whole placenta ED13: 61,2±31,2 ED15: 90,26±43,67 ED17: 104,94±76,13 HPZ: ED13: 106±56 ED15: 139±55 ED17: 172±85 LPZ: ED13: 50±31 ED15: 73±39 ED17: 75±37	N/A
FRIAS ET AL 2014 [65]	1 rhesus monkey (G133)	Gd-CA	3 T T1-weighted 2D gradient echo sequence	Gamma Capillary Transit Time (GCTT) model	Volumetric flow rates: 25.26±10.3 mL/min	N/A
BADACHAPE ET AL 2019 [36]	24 FPU at E14.5, 20 FPU at E16.5, 23 FPU at E18.5 Mice	Liposomal-Gd	1T T1-weighted 3D gradient-recalled echo sequence (T1w-GRE)	Steepest slope model	N/A	E14.5: 0.47 ± 0.06 E16.5: 0.5 ± 0.04 E18.5 : 0.52 ± 0.04

Table 1

ARTICLE	CONDITIONS CONTRAST AGENT	POPULATION	IMAGING SEQUENCE	TYPE OF ANALYSIS	F ($ML*MIN^{-1}1*100ML^{-1}$) MEAN ± SD		VB (%)
SALOMON ET AL 2005 [71]	Pharmacological model of preeclampsia Gd-CA	10 Noradrenaline mice 10 control mice (ED16)	1.5T 2D fast spoiled gradient echo monoslice sequence with double echo time	One-compartmental model	Control group: 72±84*	Noradrenaline group: 126±54*	N/A
LEMERY ET AL 2018 [72]	Biological model of preeclampsia Gd-CA	18 L-NAME rats 12 control rats (ED16)	4.7T DCE- spoiled gradient echo	Single-compartmental model	Control group: Fetal layer: 301±188 Maternal layer: 124±95	L-NAME group: Fetal layer: 302±169 Maternal layer:127±81	Control group: Fetal layer: 50±9* Maternal layer: 42±9* L-NAME group: Fetal layer: 56±13* Maternal layer: 49±13*
ALISON ET AL 2013 [68]	Surgical pathological model of IUGR Gd-CA	12 rats (ED19)	4.7T 2D spoiled gradient echo sequence (fast low-angle shot, FLASH)	Single-compartmental model	Non-ligated horn: Inner layer: 215±154* Outer layer 117±76*	Ligated horn: Inner layer: 116±57* Outer layer: 66±37*	Non-ligated horn: Inner layer: 41±12* Outer layer: 35±10* Ligated horn: Inner layer: 30±7* Outer layer: 26±7*
DROBYSHEVSKY ET AL 2015 [73]	Surgical ischemia model Gd-CA	Rabbit (ED25)	3T T1-weighted spoiled gradient echo sequence	Steepest slope model	Baseline phase: 77±7 *	Reperfusion-reoxygenation phase: 44±6*	N/A
ARTHUIS ET AL 2018 [75]	Surgical ischemia model Gd-CA	9 rats (ED19)	9.4T T1-weighted spoiled gradient echo sequence	Bi-compartmental model	Non-ligated horn: 90.9 mL/min/100 mL (IQR 85.1–95.7)*	Ligated horn: 51.2 mL/min/100 mL (IQR 34.9–54.9)*	Control group: 18±5 Ligated horn: 12±4

REMUS ET AL 2018 [74]	Stress-acoustic model	20 mice (ED14.5.16.5)	7T Dual-echo 3D T1-weighted gradient-echo sequence	Steepest slope model	Control HPZ: ED14.5: 147±31* ED16.5: 141±29* LPZ: ED14.,5: 56±19* ED16.5: 83±20*	Cases HPZ: ED14.5: 123±21* ED16.5: 192±51* LPZ: ED14.5: 43±12* ED16.5: 107±31*	N/A
DELOISON ET AL 2012 [41]	Surgical pathological model of IUGR SPIO (Ferucarbotran)	32 rats	1.5T 2D fast spoiled gradient-echo multisection (FSPGR)	Single-compartmental model	Non-ligated horn: 159.4 ± 54.6*	Ligated horn: 108.1 ± 41*	Non-ligated horn: 39.2 ± 11.9% Ligated horns: 42.8 ± 16.7%

Table 2

	THREE-COMPARTMENT PHARMACOKINETIC MODEL	STEEPEST SLOPE MODEL
TYPE OF PERFUSION ANALYSIS	Quantitative	Quantitative
CHARACTERIZATION OF : - WASH-IN - MICRO-CIRCULATION - WASH-OUT	 - yes - yes - yes	 - yes - no - no
DISTINCTION BETWEEN HIGH AND LOW-FLOW COMPARTMENTS	difficult	easier
ADVANTAGES	- precise	- simple - numerical robustness (low standard deviation)
DRAWBACKS	- complex - high standard deviation	- choice of AIF - underestimation of 33% of the perfusion
STUDIES	[66,67,68,71,72]	[63,69,70,73,74]

Table 3

	GD-CA (GADOTERATE-MEGLUMINE)	LIPOSOMAL-GD	SPIO	
			FERUCARBOTRAN	FERUMOXYTOL
BASIC ELEMENT	Gadolinium	Gadolinium + liposomal nanoparticle	Iron oxide	
MOLECULE DIAMETER	1nm	100nm	60nm	30nm
MOLECULAR COMPOSITION	Free gadolinium chelate	Preparation procedure described by Ghaghada [19]	Iron oxide core + carboxydextran coat	Iron oxide core + carboxymethyl-dextran coat
RELAXOMETRIC PROPERTIES AT 1,5T, ,37°C IN WATER (L.MMOL–1.SEC –1-	R1=3.6 R2=4.3	Nanoparticle-based T1 relaxivity of 35000 with dual-Gd liposomal agents	R1= 20 R2= 185	R1=15 R2=85
ELIMINATION PLASMA HALF LIFE	1.6h	18-24h	rapid initial intravascular phase (half-life 3.9–5.8 minutes), and a second distribution phase of 3 hours	14h
EXCRETION	Renal	Elimination from blood by the reticulo-endothelial system. Clearance by the liver and spleen	Stored with the body's iron reserve and used in hemopoesis. Coating with renal and faecal excretion	

Table 4